

# Characterization of Microtubule–Phosphofructokinase Complex: Specific Effects of MgATP and Vinblastine<sup>†</sup>

Beáta G. Vértessy,<sup>‡</sup> János Kovács,<sup>§</sup> Péter Löw,<sup>§</sup> Attila Lehotzky,<sup>‡,||</sup> Attila Molnár,<sup>‡</sup> Ferenc Orosz,<sup>‡</sup> and Judit Ovádi<sup>\*,‡</sup>

*Institute of Enzymology, Biological Research Center, Hungarian Academy of Sciences, Budapest, H-1518, P.O.B. 7, Hungary, and Department of General Zoology, Faculty of Sciences, University of Eötvös Loránd, Budapest, H-1445, P.O.B. 330, Hungary*

*Received September 17, 1996; Revised Manuscript Received November 20, 1996<sup>®</sup>*

**ABSTRACT:** Phosphofructokinase interacts with both microtubules and microtubules containing microtubule-associated proteins to produce bundling and periodical cross-bridging of tubules. Immunoelectron microscopy using anti-phosphofructokinase antibodies provided direct evidence that the kinase molecules are responsible for the cross-bridging of microtubules. Limited proteolysis by subtilisin, a procedure that cleaves the N-terminal segment of the free enzyme as well as the C-terminal “tails” of tubulin subunits exposed on microtubules, showed that while phosphofructokinase becomes resistant, tubulin retains sensitivity against proteolysis within the heterologous complex. These data suggest that the N-terminal segment of the enzyme, but not the C-terminal “tail” of tubulin subunits, is involved in the interaction between the microtubule and the kinase. The phosphorylation of phosphofructokinase or microtubules containing microtubule-associated proteins by the cAMP-dependent protein kinase did not interfere with the heterologous complex formation. MgATP prevents phosphofructokinase binding to the microtubules, and it can displace the enzyme from the single microtubules. However, the bundled microtubules are apparently resistant to the MgATP dissociation effect. Modelling of the assembly process suggests that the tubulin–kinase complex is able to polymerize as the free tubulin. Vinblastine, an anti-mitotic agent, inhibits tubulin assembly; however, its inhibitory effect is partially suppressed in the presence of phosphofructokinase. Fluorescence anisotropy measurements indicated that kinase and vinblastine compete for tubulin binding with no evidence for ternary complex formation. This competitive mechanism and the ability of the tubulin–enzyme complex to polymerize into microtubules may result in the resistance of the tubulin–enzyme complex against the inhibition of assembly induced by vinblastine. Microtubules formed in the presence of vinblastine plus phosphofructokinase can be visualized by electron microscopy. A molecular model is suggested that summarizes the effects of MgATP and vinblastine on the multiple equilibria in the tubulin/microtubules/phosphofructokinase system.

Microtubules are ubiquitous cellular structures involved in several essential functions of the cell (Bershadsky & Vasiliev, 1988) such as the extension and guidance of neurons at the growth cone (Sabry et al., 1991) and the formation of the mitotic spindle required for chromosomal segregation. The stability and spatial arrangement of microtubules are modified by microtubule-associated proteins (MAPs)<sup>1</sup> and a variety of other proteins that can interact with microtubules and enhance the formation of bundles (MacRae, 1992). In most of these cases, the bundles are loosely organized, and *in vivo* bridging elements have not been

structurally identified. Tubulin polymerization as well as MAP–microtubule interactions may be influenced by phosphorylation of both tubulin and MAPs on multiple sites by different protein kinases (Brugg & Matus, 1991; Burns et al., 1984; Diaz-Nido et al., 1990; Goedert et al., 1994; Luduena et al., 1988; Serrano et al., 1987; Wandosell et al., 1986, 1987).

Extensive binding of many, but not all, glycolytic enzymes from muscle to tubulin as well as to MAP-free microtubules has been documented. In addition, subcellular particle associated activities of several glycolytic enzymes from brain homogenate or synaptosomes have been reported; however, only PFK showed considerable association even at physiological salt concentration [see Knull (1990) and references cited therein]. In *in vivo* experiments, PFK was identified in axonal transport as slow component b (SCb) with several other enzymes of intermediary metabolism which were organized as a discrete macromolecular cellular entity (Brady, 1982; Oblinger et al., 1988).

The activity and regulatory properties of muscle type phosphofructokinase-1, catalyzing the reaction: fructose 6-phosphate + ATP  $\leftrightarrow$  fructose 1,6-diphosphate + ADP, are dependent on the self-association state of the enzyme as well as on macromolecular interactions with cellular structural elements. The single active species is the tetrameric form of the enzyme. The binding of the enzyme to F-actin

<sup>†</sup> This work was supported by grants from the Hungarian National Science Foundation, OTKA (T-5412, T-6349, and T-17830 to J.O., T-2227 to J.K., and F-17392 and F-020862 to B.G.V.).

\* To whom correspondence should be addressed. Phone: +361 166 5633. Fax: +361 166 5465. E-mail: ovadi@enzim.hu.

<sup>‡</sup> Hungarian Academy of Sciences.

<sup>§</sup> University of Eötvös Loránd.

<sup>||</sup> On leave from Chemical Works of Gedeon Richter LTD., P.O.B. 27, Budapest, H-1475, Hungary.

<sup>®</sup> Abstract published in *Advance ACS Abstracts*, February 1, 1997.

<sup>1</sup> Abbreviations: FITC, fluorescein isothiocyanate; MAP, microtubule-associated protein; PFK, phosphofructokinase; PKA, cAMP-dependent protein kinase; SDS/PAGE, sodium dodecyl sulfate/polyacrylamide gel electrophoresis; T, tubulin; VBL, vinblastine; EGTA, ethylene glycol bis( $\beta$ -aminoethyl ether)-N,N,N',N'-tetraacetic acid; PMSF, phenylmethanesulfonyl fluoride; U, units of enzymatic activity (one unit converts one micromole of substrate per minute).

stabilizes this oligomeric form [for review, see Somero and Hand (1990)]; it decreases the  $K_{0.5}$  for fructose 6-phosphate, increases the  $K_i$  for MgATP, and virtually abolishes allosteric regulation by glucose 1,6-bisphosphate and fructose 1,6-bisphosphate (Beitner, 1990). Phosphorylation of PFK by the cAMP-dependent protein kinase (PKA) is also dependent on the oligomeric state of PFK; however, it affects the activity of the enzyme only slightly (Zhao et al., 1991). Previously, we have shown that dimeric PFK binds to the tubulin dimer, MAP-free or MAP-containing microtubules. The affinity of the kinase toward microtubules is lower ( $K_d = 1 \mu\text{M}$ ) than toward tubulin dimer ( $K_d = 0.3 \mu\text{M}$ ) (Lehotzky et al., 1993). The presence of MAPs does not interfere with PFK binding to tubules (Vértessy et al., 1996). The specific binding of the inactive dimeric kinase decreases the overall activity of this key glycolytic enzyme since the equilibrium between the inactive dimer and the active tetramer is shifted (Lehotzky et al., 1993).

Electron microscopic studies provided evidence for the bundling of microtubules by glyceraldehyde-3-phosphate dehydrogenase (Durrieu et al., 1987b; Huitorel & Pantaloni, 1985; Somers et al., 1990) and PFK (Lehotzky et al., 1994). The bundling process in both cases was inhibited by ATP (Huitorel & Pantaloni, 1985; Lehotzky et al., 1994; Somers et al., 1990). The detailed morphological studies revealed periodic cross-bridges of microtubules induced by PFK: three to four closely aligned tubules are connected by rows of highly periodic lateral arms about 13 nm long and 12 nm wide (Lehotzky et al., 1994).

Microtubules formed by assembly of tubulin dimers are labile in many cell types, and some of their functions depend on this lability. The lability can be seen in their extreme sensitivity to various drugs. Several synthetic and natural compounds that specifically interact with tubulin or microtubules are important in the dissection of the properties and functions of microtubules. Vinblastine (VBL), a dimeric *Catharanthus* alkaloid, can bind to tubulin, to microtubule ends, or to nonmicrotubular tubulin aggregates, as well, with differing affinities. VBL destroys microtubule function; the molecular mechanisms responsible for this effect of the drug depend on the concentration of the drug and include perturbation of microtubule dynamics, inhibition of microtubule assembly, and induction of the formation of aberrant tubulin oligomers (e.g., spirals, paracrystals) (Wilson & Jordan, 1994). The binding site of a fluorescent VBL analogue was recently localized on  $\beta$ -tubulin (Rai & Wolff, 1996). In contrast to VBL, taxol, that binds to the tubulin polymer, enhances and stabilizes microtubule formation (Parness & Horowitz, 1981). The binding sites for VBL and taxol on the microtubule are different (Correia, 1991), although taxol also binds to the  $\beta$ -tubulin subunit, as shown by photoaffinity labeling with taxol derivatives (Rao et al., 1994, 1995). At high taxol concentrations, microtubule mass increases sharply and dynamics are almost completely suppressed (Derry et al., 1995; Wilson et al., 1974) since taxol binds to terminal tubulin subunits before they dissociate from the microtubule end (Caplow et al., 1994). The binding of taxol to tubulin does not induce any qualitative changes in the mechanism of polymerization, and the intermolecular contacts remain the same as in the native microtubules (Howard & Timasheff, 1988). Our recent quantitative electron microscopic data of taxol-stabilized microtubule geometry also suggested that the native-like microtubule

organization is not perturbed by taxol (Lehotzky et al., 1994). For these reasons, taxol is routinely used to induce polymerization and for stabilization of microtubules.

In this paper, we reinforce that in the presence of PFK microtubules form bundles by rows of lateral projections, and we provide immunoelectron microscopic evidence for the localization of the kinase on the cross-bridged tubules. We ascertain and investigate the effects of the ligands, MgATP and VBL, as well as phosphorylation on the homologous and heterologous associations in tubulin–microtubule–PFK systems. A molecular model is presented that is based on the results obtained in various experimental systems.

## MATERIALS AND METHODS

**Materials.** PFK from rabbit muscle, taxol, and porcine heart PKA catalytic subunit were obtained from Sigma. MgATP was purchased from Boehringer, GTP from Aldrich. VBL was kindly provided by Richter Gedeon Rt., Budapest, Hungary. All other chemicals were reagent-grade commercial preparations. The crystalline suspension of PFK was centrifuged at 10000g for 5 min. The pellet was suspended in HEPES buffer (50 mM Hepes, pH 7.0, containing 100 mM KCl, 2 mM dithioerythritol, and 5 mM  $\text{MgCl}_2$ ), and then the enzyme was dialyzed against the same buffer.

Protein concentrations were determined spectrophotometrically, using a molar absorption coefficient of  $1.03 \times 10^5 \text{ M}^{-1} \text{ cm}^{-1}$  at 276 nm for tubulin (Na & Timasheff, 1986) and  $8.88 \times 10^4 \text{ M}^{-1} \text{ cm}^{-1}$  at 280 nm for PFK (Hesterberg & Lee, 1982). Molar concentrations of tubulin dimer and PFK monomer were used in all calculations (unless otherwise stated) based on molecular weights of 100 000 (Little & Seehaus, 1988) and 83 000 (Luther et al., 1986), respectively. The protein concentration of MAP-free or MAP-containing microtubules was determined by Bradford's assay (Bradford, 1976) using bovine serum albumin as standard; it is given in units of milligrams per milliliter.

**Discontinuous sodium dodecyl sulfate/polyacrylamide slab gel electrophoresis** in 7.5 or 9% polyacrylamide gels (SDS/PAGE), as described by Laemmli (1970), was used to follow protein purification, the composition of the pellets and supernatants, and the time course of limited proteolysis. After electrophoresis, proteins in the gel were fixed in 50% (v/v) methanol–7% (v/v) acetic acid. Gels were stained in 0.5% (w/v) Coomassie Brilliant Blue dissolved in 50% (v/v) methanol–7% (v/v) acetic acid for 1 h at room temperature, and destained in 25% methanol–10% acetic acid.

**PFK Activity Assay.** 2  $\mu\text{M}$  (0.16 mg/mL) PFK together with MgATP at various concentrations (0.01–5 mM) was preincubated with or without 1 mg/mL microtubule in HEPES buffer at 30 °C for 30 min. Enzyme activity was assayed at 1.6  $\mu\text{g/mL}$  PFK concentration in 50 mM Tris buffer, pH 8.0, containing 2 mM fructose 6-phosphate, MgATP at the various concentrations present in the preincubation mixtures, 3 mM  $\text{MgCl}_2$ , 0.2 mM NADH, 3 mM dithioerythritol, 0.1 mM ethylene glycol bis( $\beta$ -aminoethyl ether)-*N,N,N',N'*-tetraacetic acid (EGTA), 2 units (U) of aldolase, 12 U of triosephosphate isomerase, and 2 U of glycerol-3-phosphate dehydrogenase at 30 °C, pH 8.0 (Mayr, 1987). 20  $\mu\text{M}$  taxol did not affect the activity of PFK.

**Tubulin Preparation.** MAP-free tubulin was prepared from calf brain as described by Na and Timasheff (1986).

Purified tubulin showed no contamination with MAP when run on overloaded 7.5 or 9% polyacrylamide gels using SDS/PAGE. Tubulin was stored in 1 M sucrose, 10 mM sodium phosphate buffer, 0.5 mM  $\text{MgCl}_2$ , and 0.1 mM GTP, pH 7.0 at  $-80^\circ\text{C}$ , and dialyzed against HEPES buffer before use.

*MAP-containing microtubules* were purified from bovine brain by the taxol-stabilizing method of Vallee (1986). The preparation contained MAPs of high molecular mass (MAP1 and MAP2) as visualized on SDS/PAGE gels (7.5% polyacrylamide) (Vértessy et al., 1996). The MAP—microtubule preparation was stored in PEM buffer, pH 6.6 [0.1 M piperazine-*N,N'*-bis(ethanesulfonic acid)—NaOH containing 1 mM EGTA and 1 mM  $\text{MgCl}_2$ ] at  $6^\circ\text{C}$  and was used within 1 week after preparation; 0.1 mM phenylmethanesulfonyl fluoride (PMSF) was added during storage. All experiments involving the MAP—microtubule preparation were conducted in PEM, pH 6.8, buffer, in the presence of 100 mM KCl, 1 mM PMSF, 20  $\mu\text{M}$  taxol, and 2 mM dithioerythritol.

*Turbidity and Pelleting Measurements.* MAP-free tubulin at a final concentration of 10  $\mu\text{M}$  was incubated with or without 2 or 4  $\mu\text{M}$  PFK at different concentrations of other ligands in HEPES buffer at  $37^\circ\text{C}$ . For VBL-treated samples, tubulin was preincubated with 2  $\mu\text{M}$  VBL in the absence and presence of 2  $\mu\text{M}$  PFK. The assembly was started by addition of taxol to the samples in a final concentration of 20  $\mu\text{M}$ . Absorbance change was monitored at 350 nm by a Hewlett Packard 8451A spectrophotometer. At the times indicated in the text, the samples were centrifuged at 100000g for 20 min at  $30^\circ\text{C}$ . Under these conditions, microtubules and microtubule-bound PFK are completely pelleted, while non-microtubule-bound (uncomplexed) PFK and nonpolymerized tubulin dimers remain in the supernatant (Lehotzky et al., 1993, 1994; Vértessy et al., 1996). The protein amount in the pellet and supernatant fractions was quantified by densitometry after SDS/PAGE separation in 9% polyacrylamide gels (Vértessy et al., 1993). The precision of the determinations was better than  $\pm 10\%$ . Pelleting with 1 mg/mL MAP—microtubule was performed likewise, but with PEM, pH 6.8, buffer, containing 100 mM KCl, 1 mM PMSF, 20  $\mu\text{M}$  taxol, and 2 mM dithioerythritol, and samples were analyzed on 7.5% polyacrylamide SDS/PAGE.

*Phosphorylation and Determination of Protein-Bound Phosphate Groups.* Phosphorylation of MAP-containing microtubules and PFK by PKA was conducted in PEM, pH 6.8, buffer, together with 1 mM PMSF, 20  $\mu\text{M}$  taxol, and 2 mM dithioerythritol with the  $\text{MgCl}_2$  concentration raised to 10 mM. The phosphorylation reaction mixture contained 0.2 mM MgATP, 10  $\mu\text{g/mL}$  PKA catalytic subunit, 1 mg/mL MAP-containing microtubule, and/or 0.2 mg/mL PFK. The reaction mixture was incubated at  $30^\circ\text{C}$  for 30 min. Protein-bound phosphate groups were determined by the method of Buss and Stull (1983). The degree of phosphorylation was calculated from four independent experiments. The error of phosphate determinations was  $\pm 15\%$ .

*Rat anti-PFK was prepared* by immunizing animals with rabbit muscle PFK. Twenty-five micrograms of protein was dissolved in 250  $\mu\text{L}$  of sterile phosphate-buffered saline, and the solution was homogenized and emulsified with 250  $\mu\text{L}$  of Freund's complete adjuvant. Two subcutaneous injections, 250  $\mu\text{L}$  each, were given in the back of the animal. At 1, 2, and 3 weeks, the same injections were repeated, but with incomplete adjuvant. The animal was bled at 4 weeks;

serum was used in the experiments at different dilutions. The antibody level in the serum was checked by a standard ELISA protocol (Engwall, 1980), as described previously for tubulin antiserum (Liliom et al., 1995).

*Electron Microscopy.* For routine transmission electron microscopy, MAP-free microtubule samples were prepared as described previously (Lehotzky et al., 1994). Briefly, microtubule-containing samples were pelleted, and the pellets were prefixed (2% glutaraldehyde, 0.2% tannic acid, and 0.1 M sodium cacodylate, pH 7.4, for 1 h at room temperature). Then pellets were washed (0.1 M sodium cacodylate, pH 7.4), postfixed (0.5%  $\text{OsO}_4$  in 0.1 M sodium cacodylate, pH 7.4, 1 h at room temperature), washed, and *en bloc* stained (1% uranyl acetate, 30 min). Stained samples were dehydrated in graded ethanol and embedded in Durcupan (Fluka, Switzerland). Thin sections were contrasted with uranyl acetate and lead citrate. The specimens were examined and photographed in a JEOL CX 100 electron microscope operated at an accelerating voltage of 80 kV. Magnification was calibrated with a diffraction grating replica (2160 L/mm, Balzers).

For immunogold electron microscopy, a small pellet of MAP-free microtubules was fixed in a mixture of freshly prepared 1% formaldehyde and 0.2% glutaraldehyde in 0.1 M cacodylate buffer for 20 min. Then the pellet was washed in buffer, dehydrated in ethanol, and embedded in Durcupan. Thin sections were cut and mounted on nickel grids. The grids were floated on 5%  $\text{H}_2\text{O}_2$  drops for 5 min, washed, and blocked with 0.5% w/v non-fat dry milk power, 2% bovine serum albumin in phosphate-buffered saline for 20 min and incubated in rat anti-PFK IgG serum diluted 1:500 in 0.25% milk power, 1% bovine serum albumin in phosphate-buffered saline in a humid chamber for 12 h at  $4^\circ\text{C}$ . After being rinsed in 1% bovine serum albumin in phosphate-buffered saline, the buffer was exchanged to 0.1 M Tris-HCl (pH 8.3). Then the grids were floated on a drop of 5 nm colloidal gold conjugated goat anti-rat IgG (Sigma) diluted 1:100 in 1% bovine serum albumin, 0.25% Tween-20 in 0.1 M Tris-HCl in a humid chamber for 5 h at  $4^\circ\text{C}$ . Finally grids were washed and dried. Sections were counterstained with 2% uranyl acetate prior to examination as above. Control sections were processed as described above; however, the step of incubation in the rat anti-PFK IgG serum was omitted.

VBL-treated samples were prepared by incubating 5  $\mu\text{M}$  MAP-free tubulin, 20  $\mu\text{M}$  taxol, and 2  $\mu\text{M}$  VBL with and without 4  $\mu\text{M}$  PFK for 60 min at room temperature. These samples were investigated by *negative staining*. A drop from the unpelleted samples was applied to formvar/carbon-coated glow-discharged copper grids for 30 s. The solution was then removed and the grid stained with one drop of freshly filtered 1% aqueous uranyl acetate for 30 s. The excess of stain was removed by blotting with filter paper.

*Limited Proteolysis by Subtilisin.* MAP-free tubulin at 60–100  $\mu\text{M}$  concentration in 50 mM 2-(*N*-morpholino)-ethanesulfonate buffer, pH 6.8, containing 2 mM dithioerythritol was polymerized at  $37^\circ\text{C}$  by the addition of 20  $\mu\text{M}$  taxol, 1 mM GTP, 1 mM  $\text{MgCl}_2$ , and 1 mM EGTA. Assembly was allowed to proceed for 30 min at  $37^\circ\text{C}$ , followed by pelleting of microtubules for 20 min at 100000g centrifugation at  $30^\circ\text{C}$ . Microtubules were resuspended in 50 mM 2-(*N*-morpholino)ethanesulfonate buffer, pH 6.8, containing 100 mM KCl, 2 mM dithioerythritol, 1 mM

MgCl<sub>2</sub>, 1 mM EGTA, and 20  $\mu$ M taxol, and the concentration of the microtubule preparation was determined by Bradford's assay. Proteolysis was carried out in 50 mM 2-(*N*-morpholino)ethanesulfonate buffer, pH 6.8, containing 100 mM KCl, 2 mM dithioerythritol, 1 mM MgCl<sub>2</sub>, and 1 mM EGTA using two experimental protocols with differing protein ratios. In one set, 1 mg/mL microtubule was preincubated with or without 12  $\mu$ M (1 mg/mL) PFK at 30 °C for 30 min. Then 10  $\mu$ g/mL (1% w/w of microtubule) subtilisin was added to the samples. In the other set, 2.4  $\mu$ M (0.2 mg/mL) PFK was preincubated with or without 1 mg/mL microtubule at 30 °C for 30 min in the same buffer as above, followed by the addition of 0.2  $\mu$ g/mL (0.1% w/w of PFK) subtilisin. At different time intervals, aliquots were taken, and digestion was stopped by the addition of 1 mM PMSF. Samples were analyzed by SDS/PAGE in 7.5% polyacrylamide gels. In some cases, in order to obtain separation of  $\alpha$ - and  $\beta$ -tubulin subunits, gel electrophoresis was conducted according to Sackett et al. (1985).

**Anisotropy Measurements.** PFK or tubulin was labeled with fluorescein isothiocyanate (FITC) as described previously (Lehotzky et al., 1993). Proteins at a final concentration of 5  $\mu$ M were treated with 2–5 mg of FITC–Celite for 1 h in the dark at 4 °C in a volume of 0.5 mL. The unreacted dye was then removed by gel filtration of the clarified sample through a column of Sephadex G-25 equilibrated with HEPES buffer. The extent of fluorescein labeling was determined by measuring the absorbance of the modified protein at 490 nm, using a molar absorption coefficient of  $6.6 \times 10^4 \text{ M}^{-1} \text{ cm}^{-1}$  (Ovádi et al., 1978). The degree of labeling was  $1.0 \pm 0.2$  calculated for monomeric PFK and  $0.5 \pm 0.1$  calculated for dimeric tubulin. Fluorescence intensity and anisotropy were measured in HEPES buffer at an excitation wavelength of 470 nm and an emission wavelength of 520 nm, at 30 °C. For each measurement, at least 10 determinations of the vertically and horizontally polarized components of the fluorescent emission were made with an error of less than  $\pm 5\%$ . The anisotropy was calculated as previously described (Ovádi et al., 1978).

## RESULTS AND DISCUSSION

**Visualization of Microtubules Decorated by PFK.** In agreement with our previous observations (Lehotzky et al., 1994), electron microscopic examination of resin-embedded samples revealed that microtubules are connected by rows of highly periodic lateral arms when incubated in the presence of PFK (Figure 1a). The cross-bridging of microtubules in our experiments was not induced by taxol used for stabilization of tubules since the control sample (no PFK) did not contain bundled tubules (Lehotzky et al., 1994).

Immunoelectron microscopic studies using anti-PFK antibody were carried out to get additional evidence for the involvement of PFK in the cross-bridging of tubules. Anti-PFK antibody was visualized by a colloidal gold conjugated anti-IgG, as the second antibody. As shown in Figure 1b, the immunogold conjugates are clearly seen on microtubules and cross-bridging structures when polymerization was conducted in the presence of PFK. Nonspecific labeling by gold-linked second antibody is minimal on control sections incubated in the absence of antibody to PFK (Figure 1c), and no immunostaining is seen on microtubules polymerized without addition of PFK (data not shown). Therefore, the

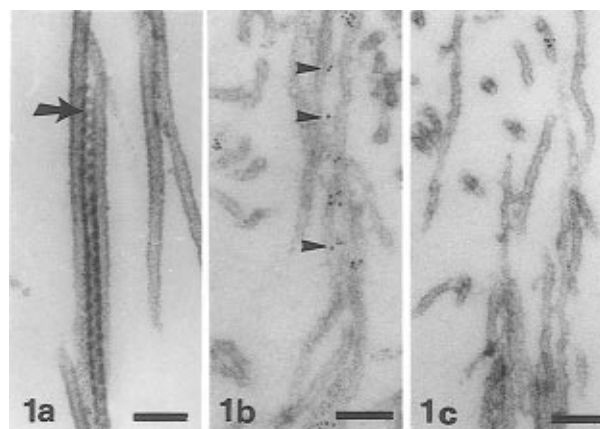


FIGURE 1: Electron microscopic images of MAP-free microtubules assembled in the presence of PFK. Panel a: Conventional processing (embedded pellet samples, glutaraldehyde–OsO<sub>4</sub> fixation, uranyl acetate and lead citrate staining). Panel b: Immunostaining for PFK [embedded pellet samples, formaldehyde/glutaraldehyde fixation, immunostaining with anti-PFK antibody (cf. Materials and Methods), uranyl acetate counterstaining]. Panel c: Section incubated in the absence of anti-PFK and then stained with gold-conjugated second antibody. Note the periodic cross-bridges (arrow) in (a) and the presence of gold conjugates on the surface of microtubules and on structures between adjacent microtubules (arrowheads) in (b) and the low level of nonspecific labeling in (c). Bar: 100 nm.

present data provide direct evidence that microtubule-bound PFK molecules are responsible for the cross-bridging of microtubules.

**Contact Surfaces Involved in Microtubule Cross-Bridging.** Muscle PFK is a dissociable oligomeric enzyme, only the tetrameric form of which is catalytically active (Uyeda, 1979). Previously we have demonstrated that it is the inactive, dimeric form which binds to microtubules (Lehotzky et al., 1993). Microtubule-bound PFK dimers associate into tetramers; however, these tetramers are inactive (Lehotzky et al., 1993, 1994). Our objective was to get information about the contact surfaces involved in the PFK–microtubule interactions and to elucidate whether similar contact surfaces stabilize the native, active tetrameric kinase and the inactive oligomeric kinase cross-bridging microtubules. Knowledge of the structural arrangement of kinase molecules contributes to the understanding of the mechanism of the highly periodic cross-bridging of tubules.

The method of limited proteolysis may be conveniently employed for studying intra- and intermolecular interactions. Since proteases preferentially attack peptide bonds exposed on the surface of proteins, their activity may be changed due to alterations in the structure of their protein substrates or steric hindrance caused by macromolecular associations.

The treatment of native PFK with subtilisin under certain limited conditions releases an N-terminal fragment of 50–60 residues (around 10 kDa) resulting in the inactivation of the tetrameric enzyme, but in this N-terminal-free PFK the tetrameric structure is retained (Gottschalk et al., 1983). The cleaved enzyme cannot bind the substrate fructose 6-phosphate or the regulatory MgATP possibly due to alteration of the relevant binding sites (Gottschalk et al., 1983).

The limited proteolysis of microtubules by subtilisin cleaves a small (around 2 kDa) C-terminal “tail” of tubulin (Paschal et al., 1989) that is exposed on the surface of microtubules and binds glycolytic enzymes [for a review, see Ovádi and Orosz (1996)]. Since PFK is more sensitive

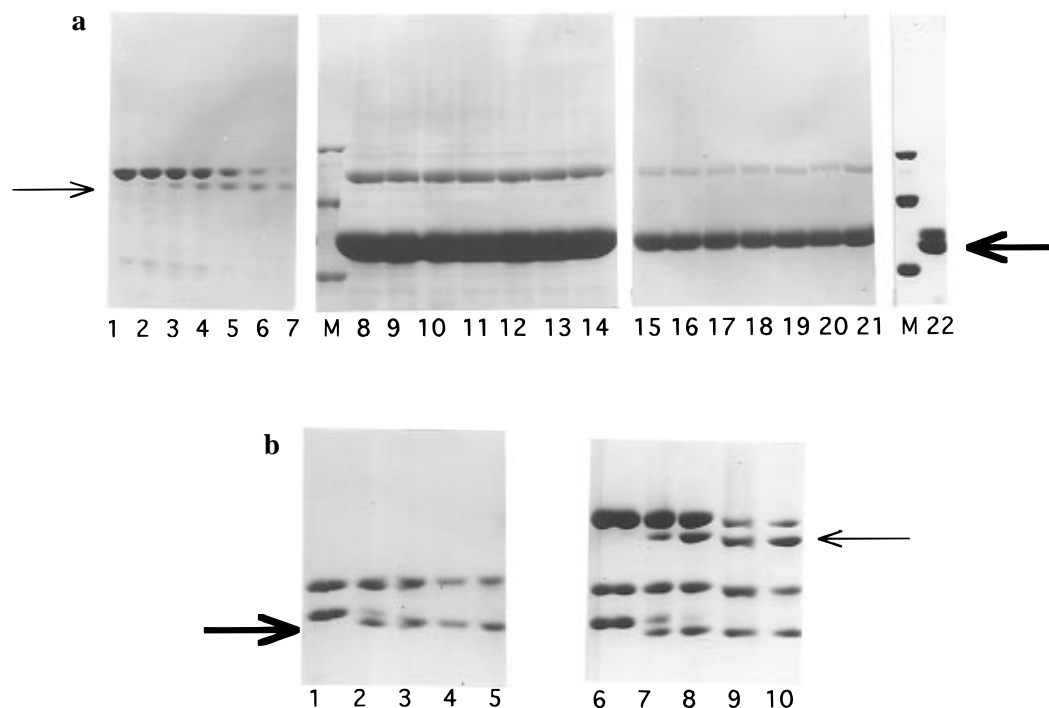


FIGURE 2: Effect of complex formation of MAP-free microtubule—PFK on limited subtilisin digestion: electrophoretic analysis. SDS/PAGE electrophoresis was conducted in a 9% polyacrylamide gel. The thin arrow indicates digested PFK; the boldface arrow indicates digested tubulin. Panel a: Protein concentrations were 1 mg/mL microtubule, 2.4  $\mu$ M (0.2 mg/mL) PFK, and 0.2  $\mu$ g/mL (10  $\mu$ g/mL in lane 22) subtilisin. Lanes 1–7 without microtubule (20  $\mu$ L aliquots loaded on the gel); lanes 8–14 and 15–21 with microtubule (20 or 4  $\mu$ L aliquots loaded, respectively) at 0, 5, 10, 30, 60, 90, and 120 min after addition of subtilisin, respectively. Lane 22: without PFK, at 10 min after addition of subtilisin, in order to visualize the expected site of the cleaved tubulin band under the SDS/PAGE conditions used in this panel. M: Marker lane with bands at relative molecular mass values of 94, 67, and 43 kDa. Panel b: Electrophoresis was carried out according to Sackett et al. (1985). Protein concentrations were 1 mg/mL microtubule, 12  $\mu$ M (1 mg/mL) PFK, and 10  $\mu$ g/mL subtilisin. Lanes 1–5 without PFK; lanes 6–10 with PFK, at 0, 5, 15, 30, and 60 min after addition of subtilisin, respectively.

to subtilisin digestion than tubulin, the cleavage of the C-terminal tubulin fragment requires significantly higher protease concentration.

In one set of experiments, PFK was digested at relatively low subtilisin concentration [1/0.2/0.0002 ratio (w/w) for microtubule/PFK/subtilisin] in the absence or presence of excess microtubule, and the kinetics of the digestion were followed by gel electrophoresis (Figure 2a). PFK and microtubule concentrations were chosen to ensure practically complete binding of PFK to the microtubule [cf. Lehotzky et al. (1993)]. In the absence of microtubule (Figure 2a, lanes 1–7), the appearance of a PFK fragment with an approximate molecular mass of 73 kDa, characteristic for the N-terminal-free PFK variant, can be visualized after 5 min digestion while in the presence of microtubule the PFK band characteristic for the intact enzyme remains unchanged up to 120 min (Figure 2a, lanes 8–14 and 15–21). Under these conditions, the intact tubulin protein band is also unchanged, no smaller fragments indicating tubulin digestion can be visualized, even if less aliquots were applied to avoid overloading of the gel (cf. Figure 2a, lanes 15–21). Subtilisin-catalyzed cleavage of tubulin would result in double bands at the tubulin position (cf. Figure 2a, lane 22, presented for ease of comparison). The observation that microtubules remain intact during this experiment (lanes 8–21) seems to exclude a potential competition between PFK and microtubules for protease action.

Figure 2b shows gel pictures of the digestion of microtubule with or without PFK at higher protease concentration [1/1/0.01 ratio (w/w) for microtubule/PFK/subtilisin]. PFK concentration was also elevated to increase the PFK-

complexed microtubule fraction. A new protein band characteristic for the “tail-free”  $\beta$ -tubulin subunit appears at 5 min of digestion; the intensity of the intact band similarly decreases and disappears at 30 min digestion in both (with or without PFK) samples. In the PFK-containing samples (lanes 6–10), the PFK fragment also appears at a relatively early stage of digestion. These data suggest that binding of PFK to microtubules does not interfere with subtilisin digestion of tubulin which targets cleavage of the C-terminal “tail” of tubulin (Paschal et al., 1989). This suggestion has been ascertained by pelleting and electron microscopic experiments performed with subtilisin-digested “tail-free” microtubules and native PFK (Vértessy et al., 1996).

The observation that in the mixture of the two proteins PFK, but not microtubule, becomes resistant against subtilisin action can be attributed to the PFK—microtubule complexation that buries the scissile peptide bond at the PFK N-terminus, but does not protect the peptide bond at the tubulin C-terminus. Consequently, the N-terminal PFK segment may be localized on or very close to the contact surface of the dimeric PFK—microtubule complex. Since it has been suggested that the N-terminal segment is not involved in the intersubunit interactions (Poorman et al., 1984), while removal of this fragment leads to loss of the substrate binding affinity (Gottschalk et al., 1983), it can be hypothesized that the contact surfaces of PFK involved in the PFK—microtubule interactions may be different from those involved in the formation of the active tetrameric species. If the intersubunit binding surfaces are exposed in the dimeric kinase—microtubule complex, this structural arrangement may ensure periodical cross-bridging of micro-

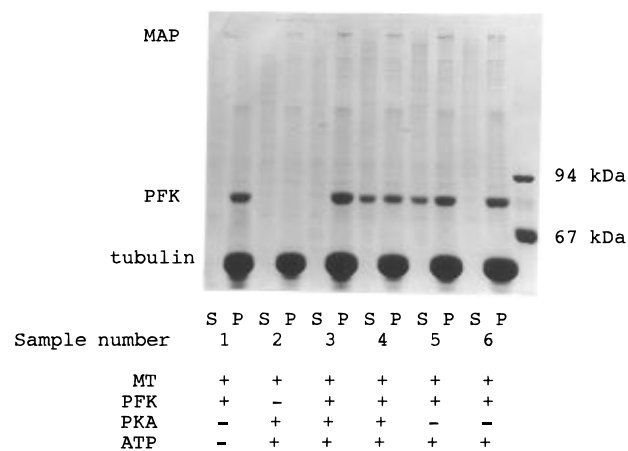


FIGURE 3: Effect of phosphorylation on PFK binding to MAP-containing microtubules: electrophoretic analysis. Samples were prepared as described under Materials and Methods; aliquots were applied on 7.5% polyacrylamide gels. Concentrations were 2.4  $\mu$ M PFK, 1 mg/mL MAP-containing microtubules, 0.2 mM MgATP, and 10  $\mu$ g/mL PKA catalytic subunit. S and P indicate supernatant and pellet fractions, respectively; sample composition is indicated by + (presence) and - (absence) signs below each sample. Microtubules and PFK were preincubated for 30 min before addition of PKA and/or MgATP, with the exception of samples 4 and 5, where PKA and/or MgATP was added to microtubules before the addition of PFK. Right lane: molecular mass markers.

tubules *via* PFK-PFK interactions. In fact, our previous electron microscopic studies indicated that four PFK monomers produce one cross-bridge (Lehotzky et al., 1994). On the other hand, bundled microtubules shield the N-terminal substrate binding site of PFK which is a plausible explanation for the lack of enzymatic activity in the tetrameric PFK species.

The above experiments show that as a result of the attachment of PFK to microtubules the enzyme becomes less sensitive to proteolysis. This may result in significant alteration in enzyme turnover. This observation exemplifies that the heteroenzyme association could have physiological relevance other than the alteration of the catalytic properties of enzymes.

**Effect of Phosphorylation on the PFK-Microtubule Interaction.** We have shown recently that MAPs do not influence PFK binding to the microtubules (Vértessy et al., 1996). Since the phosphorylation of MAPs occurring *in vivo* produces significant alteration in the conformational state of MAPs, and it can induce functional consequences in the MAP-microtubule interaction (Brugg & Matus, 1991; Burns et al., 1984), it was of interest to investigate whether phosphorylation of MAP-containing microtubules or PFK can influence their heterologous interaction. PKA, used extensively for the *in vitro* phosphorylation of MAPs, incorporates phosphate into PFK as well (Zhao et al., 1991). We chose experimental conditions for the phosphorylation of MAP-containing microtubules and PFK at which phosphorylation can be readily achieved with the uncomplexed proteins (Therkauf & Vallee, 1983; Zhao et al., 1991).

In one set of experiments, the binding of PFK to the phosphorylated MAP-containing microtubules was investigated (Figure 3, sample 4). Under our experimental conditions, phosphorylation carried out in the presence of PKA plus MgATP resulted in incorporation of 1.3 nmol of phosphate/mg of protein into MAP-containing microtubules. As shown in Figure 3, the amount of PFK pelleted with the

phosphorylated microtubules (sample 4) was less than in the control sample (sample 1); however, the difference was due to the presence of 0.2 mM MgATP that itself partially inhibits the binding of PFK to the unphosphorylated tubules [sample 5; cf. also Lehotzky et al. (1994)].

In the other set of experiments, the effect of the heterologous complex formation on the degree of phosphorylation of the interacting proteins was investigated. MAP-containing microtubules were preincubated with PFK before initiation of phosphorylation by addition of PKA plus MgATP. The total amount of incorporated phosphate was 1.8 nmol of phosphate/mg of protein, which was in good agreement with the weighted sum obtained for MAP-containing microtubule (1.3 nmol of phosphate/mg of protein) and PFK (3.7 nmol of phosphate/mg of protein) when phosphorylated separately. The simplest interpretation of this finding is that the heterologous interaction does not interfere with phosphorylation of either protein. The observation (cf. Figure 3, samples 3 and 6) that the preincubation of PFK and MAP-microtubules before addition of MgATP leads to complete pelleting of PFK with MAP-microtubules illustrates the insensitivity of the preformed PFK-microtubule complex against the ATP effect. Therefore, the effect of MgATP on the heterologous complex formation depends on the order of addition of the different components (microtubule, PFK, MgATP), questioning the reversibility of this effect in our complex system.

**Effect of MgATP on Interactions in the Tubulin-Microtubule-PFK System.** The reversibility of the MgATP effects on PFK binding to microtubules and the PFK-induced bundling of tubules was investigated by pelleting experiments and turbidity measurements, respectively. Figure 4a shows typical time courses of taxol-induced tubulin polymerization measured in the absence or presence of PFK and MgATP. The taxol-induced tubulin assembly produces microtubules similar to the native ones (Howard & Timasheff, 1988). The addition of PFK induces an additional increase of turbidity due to the cross-bridging of microtubules [cf. Figure 1 and Lehotzky et al. (1993)]. If MgATP is added to the PFK-containing tubulin solution before initiation of tubulin assembly by taxol (at 0 time), the time course is similar to that measured in the absence of PFK (cf. Figure 4a, curves a and b); i.e., no bundling is observed. However, if the bundling of microtubules by PFK was already completed, as indicated by the turbidity curve reaching its final value, and MgATP was added at 120 min, then the turbidity remained unchanged (cf. Figure 4a, curve d). When MgATP is added at an intermediate time point (at 15 min after initiation of tubulin assembly by taxol in the presence of PFK), then the increase of the turbidity is terminated, and further alteration of the absorption at 350 nm is not observed (cf. Figure 4a, curve c).

Pelleting experiments provided information for the MgATP effect on PFK binding, using the same experimental setup for incubation and MgATP addition time points as in the turbidity measurements. The centrifugation speed was chosen such that only microtubules and microtubule-bound PFK were pelleted while tubulin dimers and uncomplexed PFK remained in the supernatant. The data are summarized in Table 1. In the absence of MgATP (Table 1, line 3) or if it was added to the PFK-containing sample when the bundling was completed (Table 1, line 5), PFK sedimentation was almost complete, indicating the extensive association

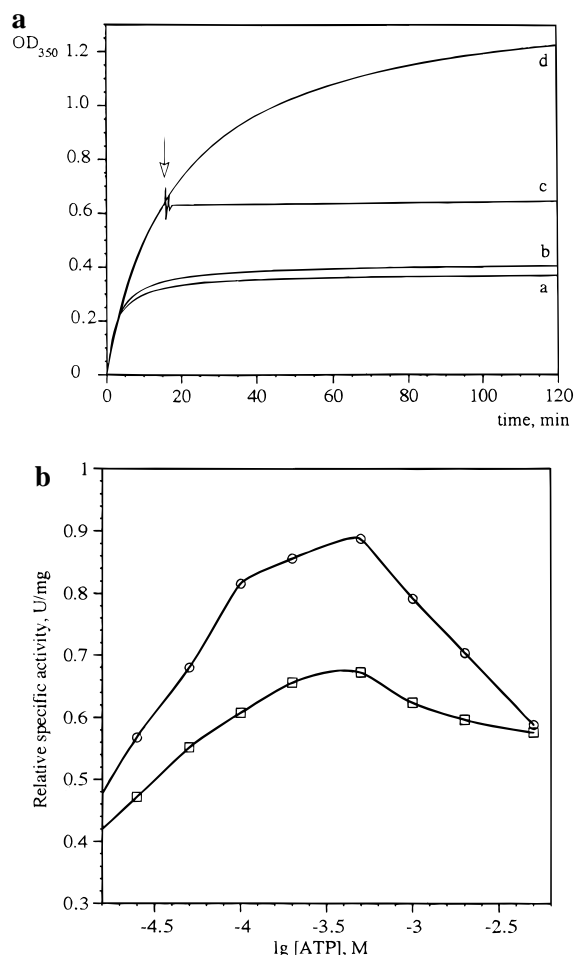


FIGURE 4: Panel a: Taxol-induced polymerization curves of MAP-free tubulin obtained by measuring the turbidity at 350 nm in the absence (a) or presence (b–d) of 2  $\mu$ M PFK with (b, c) or without (a, d) 2 mM MgATP. MgATP was added to the mixture before (b) or during the polymerization reaction (c, the arrow shows the time of MgATP addition). 10  $\mu$ M tubulin was polymerized under conditions as described under Materials and Methods. The reaction was started by the addition of 20  $\mu$ M taxol at 30 °C. Panel b: Effect of microtubules on the MgATP saturation curve of PFK. Enzyme activity was assayed at different MgATP concentrations in the absence (open circles) or presence (open squares) of 1 mg/mL microtubule under conditions described under Materials and Methods.

of PFK to microtubule under both conditions. The pelleting of microtubules was not influenced by MgATP alone. If MgATP was added to the mixture of PFK and tubulin before taxol-induced tubulin assembly, practically no PFK could be detected in the pellet (Table 1, line 4), indicating that the MgATP–PFK complex does not bind to microtubules. When MgATP was added at 15 min after initiation of tubulin polymerization in the presence of PFK and the free and bound enzyme forms were separated at 120 min, significantly less enzyme was in the pellet fractions (Table 1, line 6) than in the control sample (Table 1, line 3), however, more than when MgATP was added before tubulin polymerization (Table 1, line 4).

Both turbidity measurements and pelleting experiments showed that 2 mM MgATP totally prevents the microtubule–PFK complexation if it is added before tubulin assembly (0 time) while its addition at 115 min, when tubules are already completely cross-bridged, is ineffective. At an intermediate point of the bundling process (at 15 min), MgATP could not release completely the bound PFK from tubules. We

Table 1: Effect of MgATP and VBL on PFK Binding to Microtubules<sup>a</sup>

samples	incubation time (min)	time of MgATP addition (min)	turbidity (%)	% in pellet	
				tubulin	PFK
1. T	120	—	25	90	—
2. PFK	120	—	—	—	5
3. T+PFK	120	—	100	95	95
4. T+PFK	120	0	28	95	5
5. T+PFK	120	115	100	95	95
6. T+PFK	120	15	56	95	60
7. T+PFK	5	—	27	75	77
8. T+PFK	5	4.5	nd	74	49
9. T+PFK	15	—	53	95	83
10. T+PFK	15	14.5	nd	95	59
11. T+VBL	120	—	0	12	—
12. T+PFK+VBL	120	—	37	48	52

<sup>a</sup> The concentrations of MAP-free tubulin (T), PFK, MgATP, and VBL were 10  $\mu$ M, 2  $\mu$ M, 1 mM, and 2  $\mu$ M, respectively. 100% turbidity is defined as the absorbance at 350 nm reached after 120 min of taxol-induced polymerization of tubulin together with PFK at 30 °C. Pelleting experiments were carried out and quantified as described under Materials and Methods. The sum of the amounts of tubulin or PFK in the pellet and supernatant was taken as 100%. After the incubation time, samples were centrifuged, and pellets and supernatants were analyzed by SDS/PAGE. Data represent the average of at least three independent measurements. The error of the determinations is  $\pm 5\%$ . T stands for tubulin; nd is not determined.

interpret this partial effect of MgATP as a suggestion for the resistance of the PFK-bundled microtubule complex against the MgATP-induced dissociation. Therefore, the bundling of tubules by PFK seems to be irreversible under our experimental conditions. Nevertheless, a very slow reequilibration process in this complex system cannot be excluded. These observations, however, do not provide information for the reversibility of PFK binding to the single tubules.

The combination of the turbidity measurements and pelleting experiments showed that under our experimental conditions the taxol-induced tubulin assembly was a much faster process as compared to the bundling of microtubules; 75% and 95% of tubulin dimers were assembled into tubules within 5 and 15 min, respectively (cf. Table 1, lines 7–10), while the bundling process required greater than 2 h to attain equilibrium (cf. Figure 4a). When the bound PFK was assayed in the control samples (no MgATP), we found that at 5 min 77% of PFK sedimented (Table 1, line 7); however, the addition of MgATP at 4.5 min (just before the separation of the microtubule-bound and unbound fractions) decreased the PFK amount in the pellet to 49% (Table 1, line 8). Qualitatively similar results were obtained from the analysis of the samples at 15 min with and without MgATP (Table 1, lines 9–10). These results suggest that ATP not only prevents PFK binding to tubulin dimers but can release the bound enzyme from single tubules. The data in Table 1 allow us to estimate the rate of MgATP-induced dissociation of the PFK–single microtubule complex. The finding that the amounts of PFK in the pellets are nearly identical independently of the incubation times with MgATP (cf. Table 1, lines 6 and 10) suggests that the MgATP-induced dissociation of the enzyme is a faster process than microtubule bundling.

In order to provide independent evidence for the MgATP-induced effect, the specific enzymatic activity of PFK was

determined as a function of MgATP concentration in the absence or presence of microtubules (Figure 4b). It has been shown that MgATP, at millimolar concentrations, allosterically inhibits PFK activity, although the inhibitory concentration of MgATP is very sensitive to the assay conditions (Sols et al., 1981). Under our experimental conditions in the absence of microtubules, we find inhibition at MgATP concentrations above 0.5 mM (Figure 4b). The presence of 1 mg/mL microtubule reduces the enzymatic activity of PFK; however, the extent of the inhibition depends on the nucleotide concentration. Reduced activity of PFK in the presence of microtubule is due to the specific binding of the inactive dimers to microtubule that shifts the equilibrium between the active tetramer and inactive dimers (Lehotzky et al., 1993). At 5 mM MgATP concentration, PFK activity becomes independent of the presence of microtubule since ATP prevents heterologous complex formation. These results are in agreement with both the binding experiments and the phosphorylation experiments; i.e., MgATP was not effective in preventing PFK binding to microtubule if it was added together with PKA after 30 min of PFK–microtubule preincubation (cf. Figure 3). Therefore, we conclude that MgATP can act as a reversible modulator on PFK–microtubule complex formation as long as PFK does not form cross-bridged microtubules.

**Assembly of PFK-Bound Tubulins.** In order to clarify whether PFK-bound tubulin is able to polymerize into microtubules or the polymerization involves only uncomplexed tubulin dimers, we developed a quantitative model based on earlier calculations on tubulin polymerization [cf. Johnson and Borisy (1977); see Appendix]. The developed rate equations describe the process of tubulin polymerization in the absence and presence of PFK, assuming that PFK-bound tubulin is unable to form microtubules.

Figure 5 shows the theoretical curve of the initial rate of tubulin assembly *vs* PFK concentrations computed on the basis of eqs 5 and 8 (Appendix), with  $[T]_t = 12 \mu\text{M}$ ,  $K_a = 3.3 \mu\text{M}^{-1}$ , and  $K_a^{\text{PFK}} = 3.3 \mu\text{M}^{-1}$  (Lehotzky et al., 1993). The curve shows that the assembly rate is extensively decreased by increasing  $[\text{PFK}]_{\text{total}}$  (for symbols, see Appendix).

We also determined experimentally the initial rates of tubulin polymerization by turbidimetry at constant ( $12 \mu\text{M}$ ) tubulin and increasing (0, 2, 4, and  $11 \mu\text{M}$ ) PFK concentrations. The enzyme was added to tubulin dimers before initiation of assembly by taxol, and the preincubation time was also varied. No significant change could be observed in the assembly rate even if tubulin and PFK were preincubated for 30 min before initiation of tubulin assembly, allowing complete complex formation. As shown in Figure 5, the experimentally determined assembly rate does not change significantly upon increasing PFK concentration. Comparison of the calculated and measured data indicates that the model assuming that only PFK-free tubulin dimers are able to assemble into microtubules fails to describe the polymerization process in the tubulin/PFK system. We conclude, therefore, that the PFK–tubulin complex is able to polymerize into microtubules.

**PFK Counteracts the Effect of VBL on Tubulin Assembly.** VBL, an antimicrotubular agent, inhibits tubulin assembly at low drug concentrations because the VBL–tubulin complex caps the assembly end of microtubules [reviewed by Himes (1991)]. The inhibitory effect of VBL on tubulin

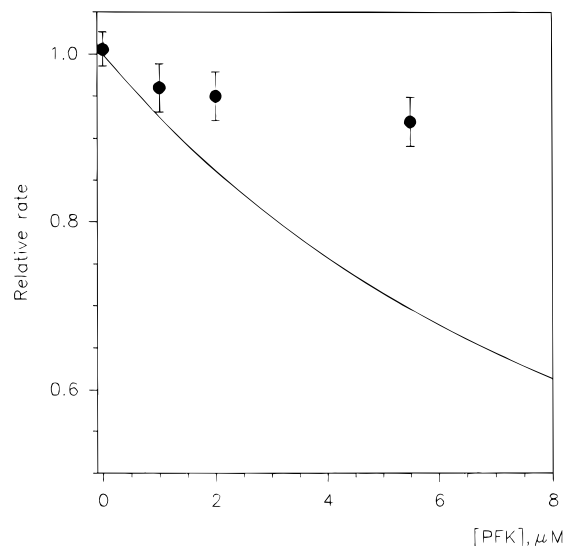


FIGURE 5: Dependence of the initial rate of MAP-free tubulin assembly on the PFK concentration. Tubulin at a final concentration of  $12 \mu\text{M}$  was incubated with or without PFK at different enzyme concentrations in HEPES buffer at  $37^\circ\text{C}$ . Initial rate of tubulin polymerization was determined from turbidity curves recorded as in Figure 4a. Data points indicate average values for three measurements, errors  $\pm 5\%$ . For other details, see Materials and Methods. The theoretical curve for the relative rate of tubulin assembly ( $v/v_{\text{control}}$ ) was calculated on the basis of eqs 5 and 8. Association constants for calculations were taken from Lehotzky et al. (1993):  $K_a = 3.3 \mu\text{M}^{-1}$  and  $K_a^{\text{PFK}} = 3.3 \mu\text{M}^{-1}$ . [PFK] stands for total PFK concentration, in dimers.

assembly counteracts the polymerizing effect of taxol. We observed that the amount of the polymerized tubulin (i.e., microtubule) depends on the ratio of the concentrations of taxol and VBL in the assay (Lehotzky et al., 1994). To assess whether the effect of VBL depends on the organization state of the tubulin/microtubule system, the PFK-induced bundling process was analyzed in the presence and absence of the drug. The VBL concentration was selected to inhibit significantly the taxol-induced tubulin polymerization in the absence of PFK (Lehotzky et al., 1994). When tubulin assembly was monitored by turbidity measurements in the presence of VBL with or without PFK, we observed that in the presence of PFK the turbidity is extensively increased, suggesting that PFK can, at least partly, overcome the inhibitory effect of VBL on tubulin polymerization (Lehotzky et al., 1994). The results of pelleting experiments are consistent with the turbidity measurements; namely, a significant fraction (48%) of tubulin dimers was assembled and pelleted if the sample contained PFK; without PFK, virtually no pelleted tubules can be detected (cf. Table 1, lines 11–12). To determine the feature of the tubulin polymer formed in the simultaneous presence of VBL, taxol, and PFK, negative staining electron microscopic studies were carried out. As shown in Figure 6, microtubules are virtually absent in the tubulin–taxol–VBL samples; however, they can be visualized when PFK has been added to the combination. A remarkable feature of both samples is that they contain many ring-like and C-shaped profiles that probably represent tubulin oligomers. However, no such profiles can be seen in samples assembled in the presence of PFK without addition of VBL (Lehotzky et al., 1994). Ring-like structures and short curved oligomeric protofilaments are common in microtubule samples under various experimental conditions including the presence of VBL [for a review, see Dustin



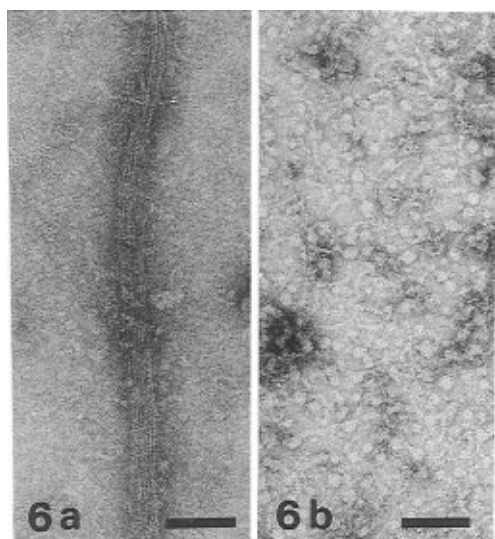


FIGURE 6: Electron micrographs of samples containing MAP-free tubulin—taxol—VBL with (panel a) or without (panel b) PFK. The samples were prepared by negative staining (no pelleting, no fixation, uranyl acetate staining; cf. Materials and Methods). Note that microtubules are present in only panel a, while both panel a and panel b samples contain numerous C-shaped and thread-like oligomers. Bar: 100 nm.

(1984) and Unger et al. (1990)]. Cryoelectron microscopic studies demonstrated that these protofilaments were particularly abundant in systems containing shrinking/disassembling microtubules (Mandelkow et al., 1991; Wade & Chrétien, 1993).

**Competitive Binding of PFK and VBL.** We hypothesized that PFK can reduce the inhibitory effect of VBL on tubulin assembly because PFK and VBL compete for tubulin binding and the PFK—tubulin complex forms microtubules but the VBL—tubulin complex does not (cf. Figure 6). The fluorescence anisotropy technique was selected to test this hypothesis since we have demonstrated that this technique is a sensitive tool for investigation of the effect of drugs on the formation of protein—protein complexes (Orosz et al., 1990; Ovádi, 1988).

In one set of experiments, unlabeled tubulin was added to FITC-labeled PFK as described previously (Lehotzky et al., 1993); in the other set of experiments, unlabeled PFK was added to FITC—tubulin, and the fluorescence anisotropy was measured in the absence or presence of 10  $\mu$ M VBL. (In both sets of experiments, the unlabeled protein was in excess in comparison to the labeled one.) As shown in Table 2, in both sets of experiments the addition of unlabeled protein to the labeled one significantly increased the anisotropy values, indicating the formation of protein—protein complexes: (labeled PFK)—tubulin and (labeled tubulin)—PFK complexes. Addition of VBL decreased anisotropy values in both cases; however, the extent of this decrease was reduced at the higher concentration of unlabeled protein. This effect was independent of which protein was labeled with the fluorescent dye. The efficiency of VBL (inhibition on formation of the tubulin—PFK complex) was decreased by increasing the unlabeled protein concentration. This finding suggests that tubulin alternatively binds to VBL or PFK and no ternary PFK—tubulin—VBL complex is formed. Therefore, the simplest explanation for the PFK-enhanced tubulin polymerization in the presence of VBL is that PFK increases the concentration of the “active” (i.e., microtubule-forming)

Table 2: Effect of VBL on the Formation of PFK—Tubulin Complex<sup>a</sup>

systems	anisotropy in presence of VBL (10 $\mu$ M)		efficiency of VBL (%)
FITC—PFK (0.01 $\mu$ M)	0.050	0.050	
+2.5 $\mu$ M tubulin	0.130	0.070	75 <sup>b</sup>
+5.0 $\mu$ M tubulin	0.155	0.150	5 <sup>b</sup>
FITC—tubulin (0.25 $\mu$ M)	0.040	0.040	
+0.6 $\mu$ M PFK	0.110	0.070	57 <sup>c</sup>
+1.6 $\mu$ M PFK	0.140	0.135	5 <sup>c</sup>

<sup>a</sup> Anisotropy measurements were carried out and calculated as described under Materials and Methods. The error of determination was  $\pm 5\%$ . The efficiencies were calculated by the following formulas: for *b*, efficiency = (anisotropy<sub>tubulin—PFK</sub><sup>x</sup> — anisotropy<sub>tubulin—PFK—drug</sub><sup>x</sup>) / (anisotropy<sub>tubulin—PFK</sub><sup>x</sup> — anisotropy<sub>PFK</sub><sup>x</sup>); for *c*, efficiency = (anisotropy<sub>PFK—tubulin</sub><sup>x</sup> — anisotropy<sub>PFK—tubulin—drug</sub><sup>x</sup>) / (anisotropy<sub>PFK—tubulin</sub><sup>x</sup> — anisotropy<sub>tubulin</sub><sup>x</sup>) where superscript *x* indicates the FITC-labeled protein.

tubulin species (free tubulin + tubulin—PFK complex); consequently, the concentration of the “inactive” tubulin—VBL complex is reduced.

Since, on one hand, PFK impedes the formation of the nonassembling tubulin—VBL complex, and, on the other hand, the formed tubulin—PFK complex is able to polymerize into microtubules, this mechanism could be responsible for the formation of tubules in the presence of the drug. Additionally, PFK, by cross-bridging microtubules, may also counteract the depolymerizing effect of VBL.

**A Molecular Model.** In previous work, we characterized the linked equilibrium of the interacting PFK—tubulin system with special emphasis on the perturbation of the association/dissociation equilibrium of PFK species by tubulin (Lehotzky et al., 1993). In this work, we focused on the association and organization of the tubulin/microtubule/PFK system as well as on the specific effects of two key ligands, MgATP and VBL. The effects of these ligands are important since MgATP is involved in many cellular events including energy production, and VBL is used extensively in cancer chemotherapy as an antimitotic agent. To summarize the results obtained from the various types of experiments, we propose the tentative molecular model presented in Figure 7, summarized as follows:

PFK stoichiometrically binds to tubulin dimers, and only each fourth tubulin dimer of microtubule binds kinase molecules due to the steric hindrance effect (Lehotzky et al., 1993). PFK-bound tubulin dimers are also able to polymerize, and the formed microtubules are periodically cross-bridged by PFK (Lehotzky et al., 1994). The cross-bridge arms are inactive tetrameric enzymes (Lehotzky et al., 1994). MgATP enhances the formation of the tetrameric PFK oligomer (Gottschalk et al., 1983). The dissociated dimeric form of PFK binds to tubulin as well as to microtubule. Consequently, MgATP expresses an inhibitory effect on the heterologous complex formation, either indirectly by inhibiting PFK dissociation into dimers or directly by its involvement in the contact surface of the microtubule—PFK complex (cf. present results obtained by limited proteolysis).

VBL binds to free tubulin and inhibits tubulin assembly. Since tubulin alternatively binds to VBL or PFK, but VBL cannot bind to the tubulin—PFK complex and the latter species is able to form tubules, this competitive mechanism



At the taxol concentrations used in our experiments, the critical concentration of tubulin is virtually zero, the disassembly rate of tubules becomes negligible, the microtubule dynamics are almost completely suppressed, and soluble tubulin is undetectable (Caplow et al., 1994; Derry et al., 1995; Lehotzky et al., 1993). Therefore, the assembly can be considered virtually irreversible, and it can be characterized in the following way:

$$d[\text{MT}]/dt = k_1[\text{T}][\text{M}] = k[\text{T}] \quad (2)$$

where  $k = k_1[\text{M}]$  is the pseudo-first-order rate constant of tubulin assembly (Burns, 1991).

Since under our experimental conditions PFK associates with tubulin dimers and the uncomplexed and the complexed protein species are in equilibrium before initiation of taxol-induced polymerization, therefore, the initial rate of tubulin assembly can be described as

$$d[\text{MT}]/dt = -d[\text{T}]/dt = k([\text{T}]_t - [\text{T-PFK}_{\text{dimer}}]) \quad (3)$$

where  $[\text{T-PFK}_{\text{dimer}}]$  is the concentration of tubulin—dimeric PFK complex and  $[\text{T}]_t = [\text{T}] + [\text{T-PFK}_{\text{dimer}}]$  is the total tubulin concentration in dimers. Since

$$[\text{T-PFK}_{\text{dimer}}] = K_a[\text{T}][\text{PFK}_{\text{dimer}}] \quad (4)$$

where  $K_a$  is the association constant of tubulin—dimeric PFK complex, the combination of eqs 3 and 4 gives

$$d[\text{MT}]/dt = k[\text{T}]_t/(1 + K_a[\text{PFK}_{\text{dimer}}]) \quad (5)$$

This formula shows that if only the free tubulin molecules are involved in the assembly process, then the presence of PFK reduces the assembly rate in a concentration-dependent manner.

Since the different oligomeric forms of PFK are in equilibrium and the dissociated forms specifically associate with tubulin (Lehotzky et al., 1993), the following constraints have to be considered:

$$K_a^{\text{PFK}} = [\text{PFK}_{\text{dimer}}]^2/[\text{PFK}_{\text{tetramer}}] \quad (6)$$

$$[\text{PFK}]_{\text{total}} = 2[\text{PFK}_{\text{tetramer}}] + [\text{PFK}_{\text{dimer}}] + [\text{T-PFK}_{\text{dimer}}] \quad (7)$$

where  $K_a^{\text{PFK}}$  is the association constant of tetrameric PFK. Both PFK and tubulin concentrations are given in dimers.

Then, the dependence of the tubulin assembly rate on PFK concentration can be calculated on the basis of eq 5 where  $[\text{PFK}_{\text{dimer}}]$  can be computed by eq 8 using the method of Wang (1995):

$$\begin{aligned} 2K_a^{\text{PFK}}K_a[\text{PFK}_{\text{dimer}}]^3 + \\ (2K_a^{\text{PFK}} + K_a + K_a^2[\text{T}]_t)[\text{PFK}_{\text{dimer}}]^2 + \\ (K_a[\text{T}]_t + 1 - K_a[\text{PFK}]_{\text{total}})[\text{PFK}_{\text{dimer}}] - [\text{PFK}]_{\text{total}} = 0 \end{aligned} \quad (8)$$

## REFERENCES

- Beitner, R. (1990) *Int. J. Biochem.* 22, 553–557.
- Bershadsky, A. D., & Vasiliev, J. M. (1988) *Cytoskeleton*, p 298, Plenum Press, New York.
- Bradford, M. M. (1976) *Anal. Biochem.* 72, 248–254.
- Brady, S. T. (1982) *Trans. Am. Soc. Neurochem.* 13, 226.
- Brugg, B., & Matus, A. (1991) *J. Cell Biol.* 114, 735–743.
- Burns, R. G. (1991) *Biochem. J.* 277, 231–238.
- Burns, R. G., Islam, K., & Chapman, R. (1984) *Eur. J. Biochem.* 141, 609–615.
- Buss, J. E., & Stull, J. T. (1983) *Methods Enzymol.* 99, 7–14.
- Caplow, M., Shanks, J., & Ruhlen, R. (1994) *J. Biol. Chem.* 269, 23399–23402.
- Chapin, S. J., Bulinski, J. C., Gundersen, G. G. (1991) *Nature* 349, 24.
- Correia, J. J. (1991) *Pharmacol. Ther.* 52, 127–147.
- Derry, W. B., Wilson, L., & Jordan, M. A. (1995) *Biochemistry* 34, 2203–2211.
- Diaz-Nido, J., Serrano, L., Lopez-Otin, C., Vandekerckhove, J., & Avila, J. (1990) *J. Biol. Chem.* 265, 13949–13954.
- Durrieu, C., Bernier-Valentin, F., & Rousset, B. (1987a) *Mol. Cell. Biochem.* 74, 55–65.
- Durrieu, C., Bernier-Valentin, F., & Rousset, B. (1987b) *Arch. Biochem. Biophys.* 252, 32–40.
- Dustin, P. (1984) *Microtubules* Springer-Verlag, Berlin, and New York.
- Engwall, E. (1980) *Methods Enzymol.* 70, 419–439.
- Goedert, M., Jakes, R., Spillantini, M. G., & Crowther, R. A. (1994) in *Microtubules* (Hyams, J. S., & Lloyd, C. W., Eds.) Wiley-Liss, New York.
- Gottschalk, M. E., Latshaw, S. P., & Kemp, R. G. (1983) *Biochemistry* 22, 1082–1087.
- Hesterberg, L. K., & Lee, J. C. (1982) *Biochemistry* 21, 216–222.
- Himes, R. H. (1991) *Pharmacol. Ther.* 51, 257–267.
- Howard, W. D., & Timasheff, S. N. (1988) *J. Biol. Chem.* 263, 1342–1346.
- Huitorel, P., & Pantaloni, D. (1985) *Eur. J. Biochem.* 150, 265–269.
- Johnson, K. A., & Borisy, G. G. (1977) *J. Mol. Biol.* 117, 1–31.
- Knull, J. R. (1990) in *Structural and Organizational Aspects of Metabolic Regulation* (Srere, P. A., Jones, M. E., & Mathews, C. K., Eds.) pp 215–228, Wiley-Liss, New York.
- Knull, H. R., & Walsh, J. L. (1992) *Curr. Top. Cell. Regul.* 33, 15–30.
- Laemmli, U. K. (1970) *Nature (London)* 227, 680–688.
- Lehotzky, A., Telegdi, M., Liliom, K., Ovádi, J. (1993) *J. Biol. Chem.* 268, 10888–10894.
- Lehotzky, A., Pálfi, Z., Kovács, J., Molnár, A., & Ovádi, J. (1994) *Biochem. Biophys. Res. Commun.* 204, 585–591.
- Lewis, S. A., & Cowan, N. (1990) *Nature* 345, 674.
- Liliom, K., Lehotzky, A., Molnár, A., & Ovádi, J. (1995) *Anal. Biochem.* 228, 18–27.
- Little, M., & Seehaus, T. (1988) *Comp. Biochem. Physiol., B: Comp. Biochem.* 90, 655–670.
- Luduena, R. F., Zimmermann, H.-P., & Little, M. (1988) *FEBS Lett.* 230, 142–146.
- Luther, M. A., Cai, G.-Z., & Lee, J. C. (1986) *Biochemistry* 25, 7931–7937.
- MacRae, T. H. (1992) *Biochim. Biophys. Acta* 1160, 145–155.
- Mandelkow, E. M., Mandelkow, E., & Milligan, R. A. (1991) *J. Cell Biol.* 114, 977–991.
- Mayr, G. W. (1987) *Methods Enzymol.* 139, 745–763.
- Na, C. N., & Timasheff, S. N. (1986) *Biochemistry* 25, 6214–6222.
- Oblinger, M. M., Foe, L. G., Kwiatkowska, D., & Kemp, R. G. (1988) *J. Neurosci. Res.* 21, 25–34.
- Orosz, F., Telegdi, M., Liliom, K., Solti, M., Korbonits, D., & Ovádi, J. (1990) *Mol. Pharmacol.* 38, 910–916.
- Ovádi, J. (1988) *Trends Biochem. Sci.* 13, 486–490.
- Ovádi, J., & Orosz, F. (1996) in *Channelling in Intermediary Metabolism* (Agius, L., & Sherratt, H. S. A., Eds.) pp 237–268, Portland Press, London.
- Ovádi, J., Salerno, C., Keleti, T., & Fasella, P. (1978) *Eur. J. Biochem.* 90, 499–503.
- Parness, J., & Horowitz, S. B. (1981) *J. Cell Biol.* 91, 479–487.
- Paschal, B. M., Obar, R. A., & Vallee, R. B. (1989) *Nature* 342, 569–572.
- Poorman, R. A., Randolph, A., Kemp, R. G., & Heinrikson, R. L. (1984) *Nature* 309, 467–469.
- Rai, S. S., & Wolff, J. (1996) *J. Biol. Chem.* 271, 14707–14711.
- Rao, S., Orr, G. A., & Horwitz, S. B. (1994) *J. Biol. Chem.* 269, 3132–3134.

- Rao, S., Orr, G. A., Chaudhary A. G., Kingston, D. G. I., & Horwitz, S. B. (1995) *J. Biol. Chem.* 270, 20235–20238.
- Sabry, J. H., O'Conner, T. P., Evans, L., Toroian-Raymond, A., Kirschner, M., & Bentley, D. (1991) *J. Cell Biol.* 115, 381–395.
- Sackett, D. L., Bhattacharyya, B., & Wolff, J. (1985) *J. Biol. Chem.* 260, 43–45.
- Schneider, F. (1981) *Naturwissenschaften* 68, 20–27.
- Serrano, L., Diaz-Nido, J., Wandosell, F., & Avila, J. (1987) *J. Cell Biol.* 105, 1731–1739.
- Shpetner, S. H., & Vallee, R. B. (1989) *Cell* 59, 421–432.
- Sols, A., Castano, J. G., Aragon, J. J., Domenech, C., Lazo, P. A., & Nieto, A. (1981) in *Metabolic Interconversion of Enzymes 1980* (Holzer, H., Eds) pp 111–123, Springer-Verlag, Berlin.
- Somero, G. N., & Hand, S. C. (1990) *Physiol. Zool.* 63, 443–471.
- Somers, M., Engelborghs, Y., & Baert, J. (1990) *Eur. J. Biochem.* 193, 437–444.
- Therkauf, W. E., & Vallee, R. B. (1983) *J. Biol. Chem.* 258, 7883–7886.
- Unger, E., Böhm, K. J., & Vater, W. (1990) *Electron Microsc. Rev.* 3, 355–395.
- Uyeda, K. (1979) *Adv. Enzymol.* 48, 193–244.
- Vallee, R. B. (1986) *Methods Enzymol.* 134, 89–127.
- Vértessy, B. G., Kovács, J., & Ovádi, J. (1996) *FEBS Lett.* 379, 191–195.
- Wade, R. H., & Chrétien, D. (1993) *J. Struct. Biol.* 110, 1–27.
- Wandosell, F., Serrano, L., Hernandez, M. A., & Avila, J. (1986) *J. Biol. Chem.* 261, 10332–10339.
- Wandosell, F., Serrano, L., & Avila, J. (1987) *J. Biol. Chem.* 262, 8268–8273.
- Wang, Z.-X. (1995) *FEBS Lett.* 360, 111–114.
- Wilson, L., & Jordan, M. A. (1994) in *Microtubules* (Hyams, J. S., & Lloyd, C. W., Eds.) pp 59–83, Wiley-Liss, Inc.
- Wilson, L., Bamberg, J. R., Mizel, S. B., Grisham, L. M., & Creswell, K. M. (1974) *Fed. Proc., Fed. Am. Soc. Exp. Biol.* 33, 158–166.
- Wilson, L., Anderson, K., & Chin, D. (1976) in *Cell Motility* (Goldman, R., Pollard, T., & Rosenbaum, J. L., Eds.) pp 1051–1064, Cold Spring Harbor Laboratory, Cold Spring Harbor, NY.
- Zhao, Z., Malencik, D. A., & Anderson, S. R. (1991) *Biochemistry* 30, 2204–2216.

BI9623441